



J. Serb. Chem. Soc. 90 (5) 593–607 (2025)
JSCS–5408

Electrochemical synthesis and anticancer inhibitory effect of copper(II)–diclofenac/decanoic acid complexes on MCF 7 breast cancer cells

HANISAH ABDUL RAHIM¹, NORAZZIZI NORDIN^{1*}, BADRUL HISHAM YAHAYA²,
YI WEN LYE¹ and AZIZUL HAKIM LAHURI³

¹School of Chemical Sciences, Universiti Sains Malaysia 11800 Gelugor, Pulau Pinang, Malaysia, ²Regenerative Medicine Cluster, Advanced Medical & Dental Institute, Universiti Sains Malaysia, Bertam, 13200 Kepala Batas, Pulau Pinang, Malaysia and ³Department of Science and Technology, Universiti Putra Malaysia Bintulu Campus, P.O. Box 396, Nyabau Road, 97008, Sarawak, Bintulu, Malaysia

(Received 24 September, revised 5 November 2024, accepted 15 February 2025)

Abstract: In this study, the Cu(II)–diclofenac/decanoic acid (Cu(II)–DF/DA) (copper(II) 2-[2-(2,6-dichloroanilino)phenyl]acetamide-decanoate) complex was synthesised using the electrochemical method by oxidising a Cu anode to release Cu²⁺, with graphite and KNO₃ serving as the cathode and supporting electrolyte, respectively. The synthesised Cu(II)–DF/DA complex underwent characterisation using ATR-FTIR, NMR, XRD and UV–Vis, confirming the success of the electrochemical synthesis. Surface morphology and particle size analyses using FESEM and TEM revealed that the synthesised Cu(II)–DF/DA complex possesses a thread-like structure with an average particle size of 4.77±1.77 nm. Subsequently, the synthesised complex was used to assess the anticancer inhibitory effects on human breast cancer (MCF 7) and normal human breast epithelial (MCF 10A) cells. The treatment of MCF 7 cancer cells with Cu(II)–DF/DA at concentrations of 25 and 100 µmol L⁻¹ resulted in a significant reduction in cell viability, with only 18 and 7 % of cells remaining viable after 72 h, respectively. In contrast, nearly 90 % of MCF 10A cells remained viable at comparable concentrations. This suggests that the synthesised Cu(II)–DF/DA shows potential as an effective and selective anticancer agent, being toxic to cancer cells while displaying lower toxicity to normal cells.

Keywords: copper(II) complex; diclofenac; electrochemical synthesis; fatty acid; nanoparticle; anticancer.

* Corresponding author. E-mail: azzizi@usm.my
<https://doi.org/10.2298/JSC240924016R>



INTRODUCTION

In recent years, the focus of chemotherapeutic research has increasingly shifted towards the investigation of non-platinum-based compounds as potential alternatives. This shift stems from the need to develop new metal-based anticancer drugs with lower toxicity. Cu has attracted considerable interest as a viable candidate due to its expected lower toxicity relative to platinum compounds. Moreover, copper complexes are compelling because of their ability to induce DNA damage, a property linked to their biologically accessible redox potential and strong affinity for nucleobases. Since the 1970s, a variety of therapeutic ligands – including thiosemicarbazones (TSCs), imidazoles and phosphines – have been incorporated into copper complexes to assess their anticancer potential.¹ According to Renfrew, the effectiveness of metal-based anticancer agents hinges on both the central metal atom and the bioactive ligand within the complex.² This is because the chemical and biological properties of the complex are significantly influenced by the donor atoms of the bioactive ligands and their characteristics.³

Diclofenac (DF, Fig. 1), also known by its IUPAC name, 2-[2-(2,6-dichloroanilino)phenyl] acetic acid, a widely used nonsteroidal anti-inflammatory drug (NSAID), is primarily known for its efficacy in treating pain and inflammation. Chemically, DF is a phenylacetic acid derivative, characterised by a benzene ring substituted with two chlorine atoms and an acetic acid moiety. Beyond its conventional use as an anti-inflammatory agent, recent research has highlighted DF's potential anticancer properties.⁴⁻⁶ The ability of DF to induce apoptosis and inhibit cell proliferation in various cancer cell lines has garnered significant attention. The anticancer effects of DF are believed to stem from its interference with the COX-2 enzyme, which is often over expressed in tumour cells and is associated with cancer progression and metastasis. According to a study conducted by Poku *et al.* (2020),⁷ the complex of DF with docosahexaenoic acid (DHA), a type of polyunsaturated fatty acid, has greater anticancer activity than their parent compound alone and the complex can be further explored for the complementary treatment of lung cancer.

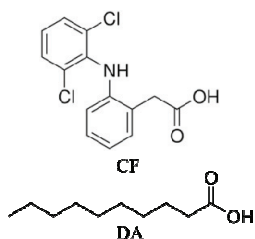


Fig. 1. Structure of DF and DA.

Fatty acids are naturally occurring monocarboxylic acids characterised by long hydrocarbon chains, which can be either saturated or unsaturated. Research has so far shown that fatty acids themselves possess antibacterial, antifungal and

anticancer properties.^{8–10} These effects are likely due to the physical interaction of fatty acids with cell membranes, where they may alter membrane permeability by interacting with the phospholipid bilayer.¹¹ The already published studies have also demonstrated that modifying fatty acids with existing anticancer drugs can enhance tissue selectivity, potentially increasing the effectiveness of chemotherapy while reducing toxicity to normal cells.^{12,13} In this study, decanoic acid (DA, Fig. 1) will be used as the fatty acid component for chemical modification with an anticancer drug. The extensive literature exists on the *in vitro* cytotoxicity of DA. Narayanan *et al.* reported that DA inhibits the proliferation of human colorectal carcinoma (HTC-116), human skin epidermoid carcinoma (A-431) and human mammary gland adenocarcinoma (MDA-MB-231).¹⁴ Additionally, Nordin *et al.* found that incorporating DA as a ligand in Cu(II) complexes produced moderate cytotoxic activity against A549 and HeLa cell lines, with IC_{50} values of 15.85 and 20.89 μM , respectively.¹⁵

Despite the promising cytotoxic activity of DF and fatty acids, there are relatively few studies on the chemical modification of DF with fatty acids available in the literature. This gap in research gave the idea for the present study, where DF was selected as the non-steroidal anti-inflammatory drug component for conjugation with decanoic acid (DA). The synthesised DF/DA was used as a ligand in the direct electrochemical synthesis of a Cu(II)–DF/DA complex. The synthesised complexes were characterised using various techniques, including ATR-FTIR, UV–Vis, NMR, XRD, FESEM-EDX and TEM. The synthesised complexes were then evaluated for their anticancer inhibitory effects on MCF 7 and MCF 10A cell lines.

EXPERIMENTAL

Chemicals and cell culture

All chemicals used were analytical grade and used without further purification. Diclofenac (DF) with 98 % purity, methanol and decanoic acid (DA) with 99 % purity were purchased from Alfa Aesar Company. Cu foil (99 % purity), ethanol (95 % purity), benzotriazole-1-yl-oxy tris (dimethylamino) (BOP reagent) with 97 % purity, dimethyl-*d*₆-sulfoxide, potassium nitrate (KNO₃), methanol and sulphuric acid were supplied from Sigma Aldrich. Acetone was purchased from EMSURE(R) ACS. Triethylamine (Et₃N) and anhydrous magnesium sulphate (MgSO₄) were supplied from Acros Organics. Dichloromethane (CH₂Cl₂), dichloromethane (extra dry), diethyl ether (99 % purity), silica chromatography and sodium hydroxide were purchased from Fisher Chemical. Human breast epithelial cell lines (MCF 10A) and human breast cancer cell lines (MCF 7) were obtained from the American Type Culture Collection (ATCC). The MCF 10A and MCF 7 cell lines were prepared in Dulbecco's modified eagle medium: nutrient mixture F-12 (D-MEM/F-12). The D-MEM/F-12 medium solution was supplemented with 1 % antibiotic (100 units mL⁻¹ penicillin and 100 $\mu\text{g mL}^{-1}$ streptomycin) and 5 % of fetal bovine serum (FBS). All cell culture reagents were purchased from Thermo Fisher Scientific.

Synthesis of DF/DA compound

The stock solution of DF and DA was prepared separately by dissolving DF (0.0740 g) and DA (0.0431 g) in 24 °C ethanol to prepare 0.01 mol L⁻¹ of concentration each. Then, a 25 mL of each stock solution was added to a 100 mL beaker. After that, 25 mL of dried CH₂Cl₂, 0.27 g of BOP reagent and 15 mL of Et₃N were added into the mixed solution. At 22 °C, the resulting solution was mixed for 2 h. After obtaining the reaction mixture, 15 mL of 0.67 % HCl_{aq} solution was added into 100 mL beaker. Then, it was extracted using CH₂Cl₂ (2×25 mL). To dry the combined organic layers, a half spatula of anhydrous MgSO₄ was added after the combined organic layers had been rinsed with 1 % HCl_{aq} solution (4×25 mL) and ultrapure water (2×25 mL). The product was then extracted using column chromatography on silica gel with a mixture of 95 % CH₂Cl₂ and 5 % methanol as the eluent. The final product was rinsed with 2 mL of diethyl ether.

Electrochemical synthesis of Cu(II)–DF/DA

An electrochemical synthesis technique was used to produce the Cu(II)–DF/DA complex. As indicated in Fig. 2, the electrolysis used a Cu foil (3×2 cm, 0.1 cm thickness) as the anode and a graphite rod as the cathode with a supporting electrolyte solution of 0.01 mol L⁻¹ KNO₃. The synthesis was carried out for 6 h using an applied voltage of 1 V. Prior to the synthesis, both the anode and the cathode were rinsed with a small amount of acetone and ultrapure water. The electrochemical synthesis was conducted using a Twintex (TP-2305TK) direct current (DC) power source. The stock solutions of previously prepared DF/DA compound were prepared by dissolving a certain amount of the compound in methanol while KNO₃ solution was prepared by dissolving the salt in ultrapure water. Then, both solutions were mixed with the volume ratio of 1:1 into the simple and undivided electrolysis cell in the 100 mL of beaker. The reaction was carried out at a temperature of 22–23 °C, with a speed of 500 rpm and initial pH 4.5. The synthesis of Cu(II)–DF/DA required 6 h to be completed. As a result, the Cu(II)–DF/DA complex will formed as a blue precipitates and will be filtered using filter paper and washed with ultrapure water and acetone several times to remove the unreacted compound, electrolyte and impurities. The precipitate was then dried in oven at 80 °C for 1 h. Melting point of DF/DA ranges 145–150 °C and Cu(II)–DF/DA 220–225 °C.

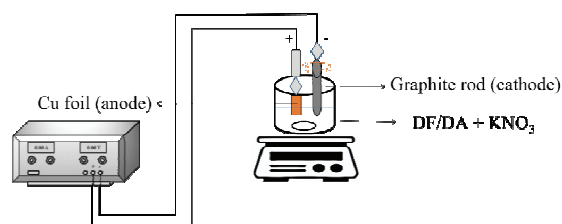


Fig. 2. Schematic diagram of the experimental set-up.

Characterisation of Cu(II)–DF/DA and DF/DA compounds

The electrochemically synthesised Cu(II)–DF/DA complex was then characterised using attenuated total reflectance – Fourier transform infrared spectroscopy (ATR-FTIR, Perkin Elmer 1310) in the range of 4000 to 600 cm⁻¹ and UV–Vis spectrophotometer (Perkin Elmer Lambda 35) in the wavelength range of 200 to 800 nm in a 10 mm quartz cuvette in ultrapure water as a reference solvent at room temperature. In addition, proton and carbon-13 nuclear magnetic resonance (¹H- and ¹³C-NMR) were carried out using the Bruker-Avance III 500

with a 500 MHz adjustment while the elemental composition of the synthesised complex was determined with an energy dispersive X-ray (EDX, Hitachi-Regulus 8220, Tokyo, Japan) with. Transmission electron microscopy (TEM, Zeiss-Libra 120, Oberkochen, Germany) with a 100 kV accelerating voltage was used to observe the nanoparticles' size and shape. Applying a drop to the grid and letting the solvent (ethanol) evaporate in the environment, the samples were prepared on carbon-coated copper grids covered with a polyvinyl formal polymer. Furthermore, an X-ray diffractometer (XRD, D8 Advance, Bruker, Billerica, MA, USA) was used to confirm the crystalline structures of the pure DF, DA and synthesised Cu(II)-DF/DA complex.

Inhibition studies

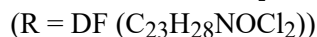
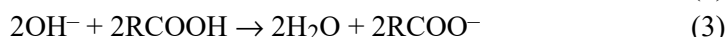
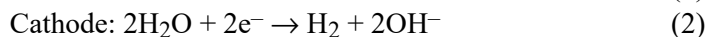
To prepare a stock solution of tested drugs (Cu(II)-DF/DA complex, DF/DA and DF (control)), the tested compounds were dissolved separately in a certain volume of dimethyl sulfoxide (DMSO). Then, mixed the 10 % of drugs and 90 % of media into the each well plate. The cells were seeded at a density of 1×10^5 cells per mL in a 96-well flat-bottomed microplate. After that, the cells were incubated at 37 °C in a 5 % CO₂ environment at different hours (24, 48 and 72 h). The cell viability assay 3-(4,5-dimethylthiazol-2-yl)-2,5-diphenyl-2H-tetrazolium bromide (MTT) was used to examine the inhibition effect on MCF 10A and MCF 7 cells upon treatment with three different compounds (DF/DA, Cu(II)-DF/DA and DF (control)) at two different concentrations (25 and 100 $\mu\text{mol L}^{-1}$). The medium in each well was removed when the cells were 70 to 80 % confluent and it was replaced with a medium containing the drugs above with two different concentrations, which are 25 and 100 $\mu\text{mol L}^{-1}$. When the treatment period was over, the medium that contained the drugs was discarded and a fresh medium that included 10 μL of MTT reagent was added to each well. The described method was performed three more times. After that, the optical density (OD) of the cells was determined using the FLUOstar Omega microplate reader (BMG Labtech, Ortenberg, Germany) at wavelengths from 570 to 620 nm.

RESULTS AND DISCUSSION

Synthesis of DF/DA and Cu(II)-DF/DA

Fig. 3 shows the proposed chemical reactions used in the synthesis of DF/DA compound. According to Chrzanowska et al., the interaction of DF drug and DA can only occur on the NH moiety of drug molecules by forming an amide bond with the carbonyl group of DA.¹³

Eqs. (1)–(4) describe the mechanism responsible for the electrochemical technique of Cu(II)-DF/DA:



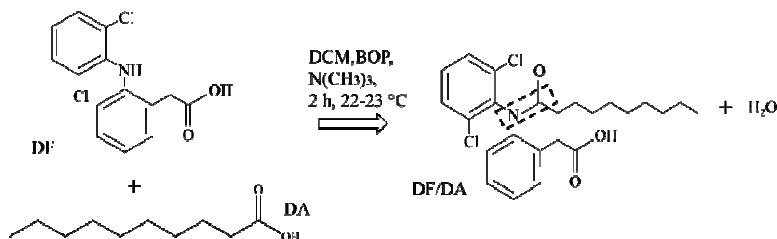


Fig. 3. Proposed chemical reaction of DF/DA synthesis.

According to the mechanism in Eq. (1), the release of Cu^{2+} from electrochemical oxidation of the Cu anode is required for the formation of Cu(II)-DF/DA complex. The electrolysis conditions should be optimised in order to get the optimal conditions for the synthesis of Cu(II)-DF/DA complex. The electrolysis conditions investigated included the type of the applied voltage, the supporting electrolyte concentration and the pH solutions. Therefore, it is expected that this optimisation research will produce the most Cu(II)-DF/DA and the least amount of Cu anode waste.

The positively charged Cu anode was electrochemically oxidised in the aqueous phase to generate Cu^{2+} (Eq. (1)). At the negatively charged graphite cathode, OH^- was formed by water reduction (Eq. (2)) and immediately interacted with DF and DA to produce $\text{C}_{23}\text{H}_{28}\text{NOCl}_2\text{COO}^-$ (Eq. (3)) in aqueous phase. The interaction of Cu^{2+} with DF/DA ions led to the formation of a blue precipitate of Cu(II)-DF/DA complex in the organic phase (Eq. (4), Fig. 4).

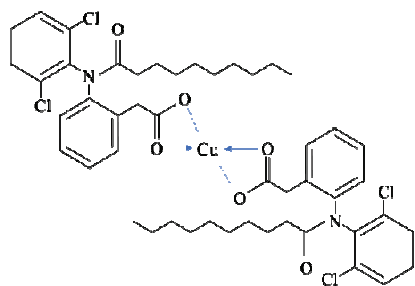


Fig. 4. Proposed structure of Cu(II)-DF/DA .

Characterisation of DF/DA and Cu(II)-DF/DA

ATR-FTIR spectroscopy. The ATR-FTIR spectrum of DF (Fig. 5) revealed an absorption peak at 3400 cm^{-1} , corresponding to the secondary amino group.¹⁶ Additionally, strong peaks observed at 1610 and 1570 cm^{-1} were attributed to the C=O stretching and the C=C stretching in the aromatic ring, respectively, within the DF structure.¹⁷ In the ATR-FTIR spectrum of DA, a prominent peak at 1698 cm^{-1} was identified, representing the stretching vibration of the carboxyl group in the fatty acid.¹⁵ Moreover, several peaks in the $2800\text{--}3000\text{ cm}^{-1}$ range indi-

cated the asymmetrical (ν_{as}) and symmetrical (ν_s) stretching vibrations of the methyl and methylene groups in the DA carbon chain, respectively.¹⁸ Similar peaks present in both the DF and DA spectra were also observed in the DF/DA spectrum (Fig. 5), confirming the formation of the DF/DA conjugate. The disappearance of the secondary amino group peak at 3400 cm^{-1} in the DF spectrum suggested the successful formation of an amide bond between the secondary amine in DF and the carbonyl group in DA, indicating that the DF/DA conjugate was successfully synthesised. After the formation of the Cu(II)–DF/DA complex, the ATR-FTIR spectra still exhibited several characteristic peaks of the DF/DA compound.

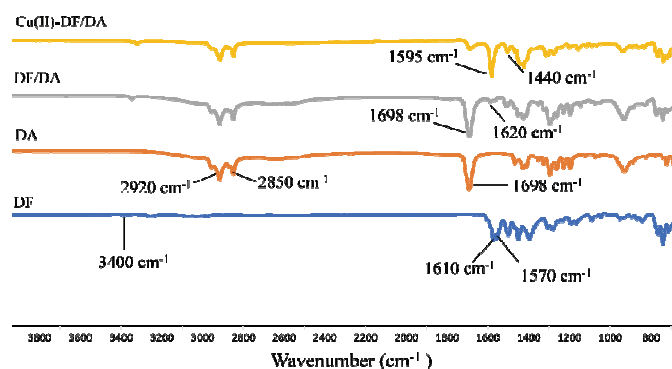


Fig. 5. ATR-FTIR spectra of: a) DF, b) DA, c) DF/DA and d) Cu(II)–DF/DA.

NMR spectroscopy. The $^1\text{H-NMR}$ spectrum of DF/DA (Fig. 6) revealed that all of the proton peaks could be observed in both the DF (Fig. S-1 of the Supplementary material to this paper) and the DA (Fig. S-2 of the Supplementary material) spectrum. Furthermore, this study observed the same proton peaks as those found in earlier studies by Yoko *et al.*¹⁹ ($^1\text{H-NMR}$ spectrum of DA) and Suhara *et al.*²⁰ ($^1\text{H-NMR}$ spectrum of DF) when compared. The proton that connects to the nitrogen atom in the DF structure, established as “a” in Fig. S-1 at δ_{H} of 12 ppm, was not identified in the DF/DA compound’s NMR spectrum. This is due to the fact that a proton has been substituted by the carboxyl group of DA. The OH group from the carboxyl group of DA generated water molecules with the proton that linked to the nitrogen atom in DF. As a result, at the end of the reaction, the carboxyl group of DA is attached to the nitrogen atom, forming a tertiary amide in the DF/DA compound and this reaction agrees with the proposed structural formula of the DF/DA compound that is shown in Fig. 6.

The presence of carbon in the carbonyl group of the fatty acid group was revealed by the results from the $^{13}\text{C-NMR}$ spectrum of DF (Fig. S-3 of the Supplementary material) and DA (Fig. S-4 of the Supplementary material), which were presented at δ_{C} of 172 and 176 ppm, respectively. These two peaks show

simultaneously in the spectrum of the DF/DA compound (Fig. 7), indicating that the complex contains two carbonyl groups. The carbon signals appear before δ_c of 40 ppm in the DF/DA spectrum, indicating the presence of different methyl groups, as shown in the DA spectrum, whereas carbon signals appear after δ_c of 110 ppm in the DF spectrum, indicating the presence of carbon in aromatic rings. Therefore, based on the ^1H - and ^{13}C -NMR spectra, it can be concluded that the DF/DA molecule has been successfully synthesised.

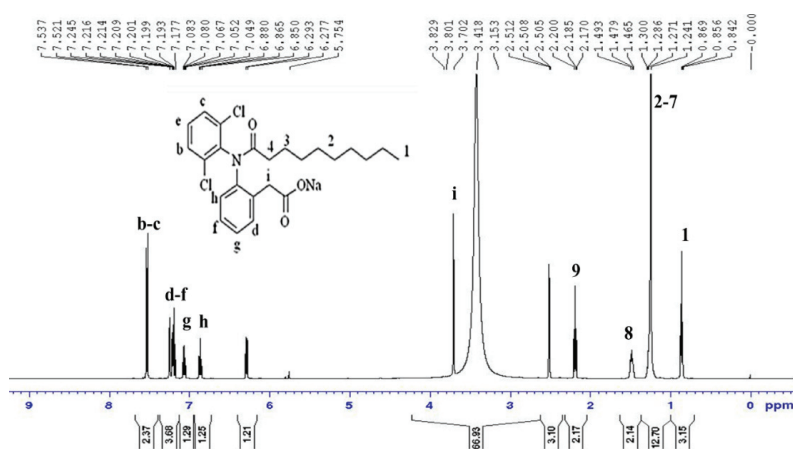


Fig. 6. ^1H -NMR spectrum of DF/DA.

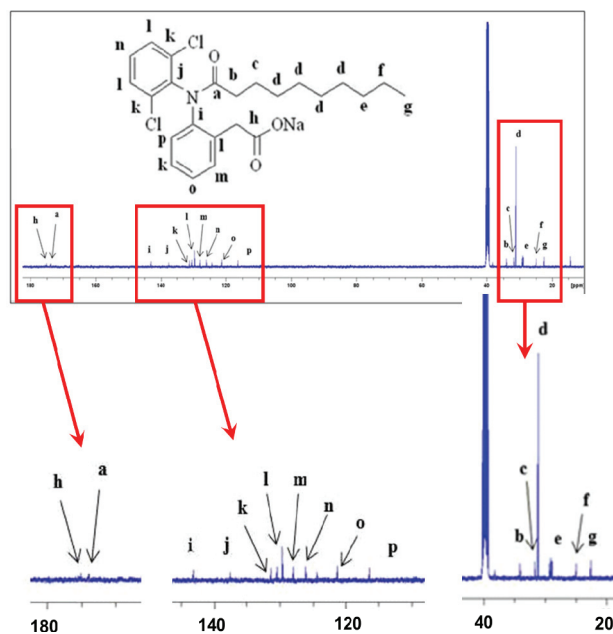


Fig. 7. ^{13}C NMR spectrum of DF/DA compound.

UV-Vis spectroscopy. The UV-Vis spectrum of the Cu(II)-DF/DA complex shows the presence of two different absorption peaks (Fig. 8). A prominent signal in the UV region at 300 nm indicates the $n-\pi^*$ transition of the carbonyl group in the DF structure.²¹ Additionally, an intense peak that can be seen in the visible region at 674 nm (Cu(II)-DF/DA) indicates the d-d transition of Cu^{2+} , as a result of a transition from the filled d level ($z^2, xy, xz/yz$) to the half-full d level (x^2-y^2).¹⁸ Without the complexation with the Cu metal centre, the UV-Vis spectrum of the DF/DA ligand displays a single absorption peak at a wavelength of 277 nm, corresponding to the $n-\pi^*$ transition of the carbonyl group in the DF structure. The shift of the UV-Vis absorption peaks of a ligand to longer wavelengths after the complexation with a transition metal centre is due to the electronic interactions between the ligand and the metal ion.¹⁸ The desired Cu(II)-DF/DA complexes have been successfully formed by the electrochemical technique that relies on the obtained spectra.

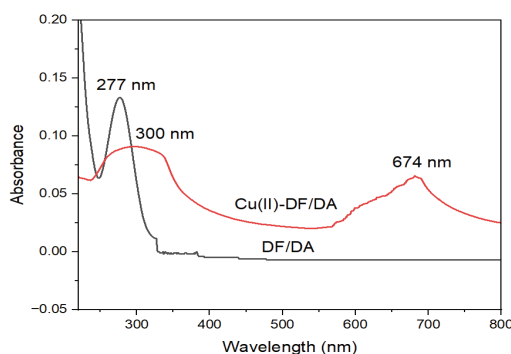


Fig. 8. UV-Vis spectra of Cu(II)-DF/DA and DF/DA compounds.

XRD. Fig. 9 shows the powder XRD patterns of DF, DA and electrochemically synthesized Cu(II)-DF/DA. All samples in Fig. 9 showed well-defined

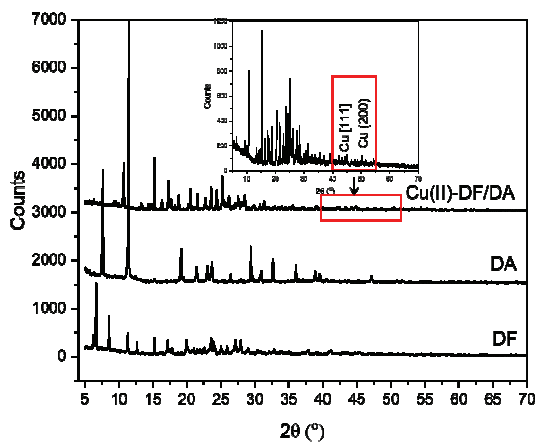


Fig. 9. XRD patterns of DF, DA and Cu(II)-DF/DA.

diffraction peaks thus proving the samples crystallized into layered structures. The main peaks indicated by the DA (at 7 and 11° at a lower angle)²² and DF (at 6, 8 and 15° at a higher angle)²³ diffractograms in this study are consistent with those reported in previous studies. Interestingly, the main peaks that exhibited the characteristic features of DF and DA are present in the Cu(II)–DF/DA diffractogram, indicating the presence of both compounds in the synthesised complex. Meanwhile, the presence of Cu in the synthesised complex is confirmed by the weak peaks observed at 44 and 50° at higher angle, corresponding to the (111) and (200) planes, respectively.

FESEM-EDX analysis. FESEM analysis was employed to investigate the surface morphology of synthesised Cu(II)–DF/DA complex. The micrograph obtained in Fig. 10a reveals that the synthesised complex exhibits a thin, thread-like structure with varying thicknesses. Meanwhile, EDX analysis was used to determine the elemental composition of the synthesised Cu(II)–DF/DA complex. The EDX spectrum in Fig. 10b demonstrated that Cu(II)–DF/DA complexes contain C, N, O, Cl and Cu. This corroborates the findings from the spectroscopy-based characterization described earlier, confirming the successful synthesis of the Cu(II)–DF/DA complex.

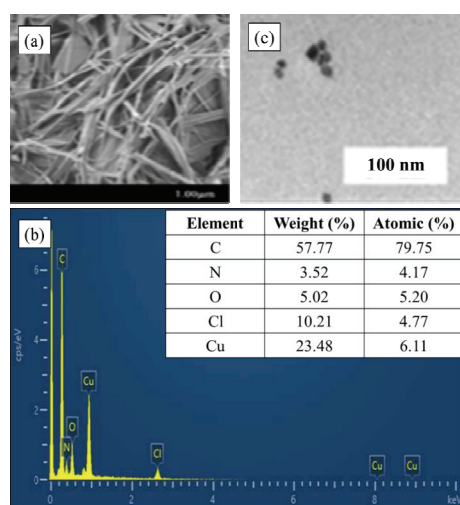


Fig. 10. a) FESEM micrograph, b) elemental composition using EDX and c) TEM micrograph of the synthesised Cu(II)–DF/DA.

Particle size. Fig. 10c illustrates the size of Cu particles in Cu(II)–DF/DA complex. When applying a low voltage (1 V) and supporting electrolyte concentration (0.01 mol L⁻¹ KNO₃) during the electrochemical synthesis of Cu(II)–DF/DA, it yields smaller CuNPs with an average size of 4.77±1.77 nm. This phenomenon can be attributed to the slow release of Cu²⁺ from the electrochemical oxidation of Cu anode into the bulk solution containing DF/DA ligand when using a low applied voltage and supporting electrolyte concentration thereby

resulting in smaller Cu particle sizes. This study has shown that the particle size of the synthesised product can be controlled by controlling the applied voltage and supporting electrolyte concentration during the synthesis process as reported by previous researchers.^{24–27}

Anticancer inhibitory effect of Cu(II)–DF/DA on MCF 7 and MCF 10A cells

The purpose of this study is to assess the inhibitory effect of Cu(II)–DF/DA on MCF 7 cells (tumour cells) and MCF 10A cells (normal cells) using the MTT assay. It was conducted to evaluate the efficacy of suppressing the tumour cell proliferation while simultaneously minimizing toxicity on normal cells following treatment with Cu(II)–DF/DA. Nevertheless, it should be highlighted here that this study focuses on the inhibitory effects of the synthesised Cu(II)–DF/DA complexes on selected cell lines at concentrations of 25 and 100 $\mu\text{mol L}^{-1}$ to assess how these concentrations affect cellular growth rather than their cytotoxic effects. The inhibitory effects of the Cu(II)–DF/DA on both cell types were depicted in Fig. 11. As a control, the inhibitory effects of the commercial DF sample and DF/DA ligand were also examined to compare the inhibitory efficiency of synthesised Cu(II)–DF/DA with that of the commercial DF and the DF/DA ligand only. Based on Fig. 10a, there was a greater inhibitory effects of Cu(II)–DF/DA on MCF 7 cells when the incubation period was extended from 24 to 72 h. The following treatment with Cu(II)–DF/DA at a concentration of 25 $\mu\text{mol L}^{-1}$, the percentage of viable cells are reduced. After 72 h of treatment, Cu(II)–DF/DA showed the strongest inhibitory effect among the samples, with significantly lower percentage of viable cells (18 %) than DF and DF/DA molecules. This suggests that the formation of complexes between Cu and the DF/DA ligand increased the toxicity of the synthesised complexes against selected cancer cells. Interestingly, after 72 h of incubation, approximately 90 % of the MCF 10A normal cells remained alive upon treatment with the tested samples, indicating low inhibitory effects and less toxicity towards normal MCF 10A cells (Fig. 11a).

The results presented in Fig. 10b demonstrate that the inhibitory effects on the selected cancer cells are enhanced when the tested sample concentration increases from 25 to 100 $\mu\text{mol L}^{-1}$. In addition, low percentage of viable cells was detected when compared to the treatment utilising a 25 $\mu\text{mol L}^{-1}$ of Cu(II)–DF/DA sample. When treated with 100 $\mu\text{mol L}^{-1}$ of Cu(II)–DF/DA, the percentage of viable cells reduced from 18 (Fig. 10a) to 7 % (Fig. 11b), indicating that synthesised complex had the most inhibitory impact among the samples on MCF 7 cells. Notably, following a 72 h treatment with 100 $\mu\text{mol L}^{-1}$ of all evaluated drugs, the vitality of normal MCF 10A cells continued to be above 90 %. Thus, there was no toxicity observed towards MCF 10A cells when the sample concentration was increased to 100 $\mu\text{mol L}^{-1}$. Importantly, the Cu(II)–DF/DA complex

demonstrated selective anticancer properties, significantly reducing cell viability in MCF7 cancer cells while showing minimal toxicity to normal MCF10A cells, suggesting its potential as an effective and targeted anticancer agent. These findings open the door for further research into copper-based complexes as selective cancer therapies with reduced side effects on healthy cells.

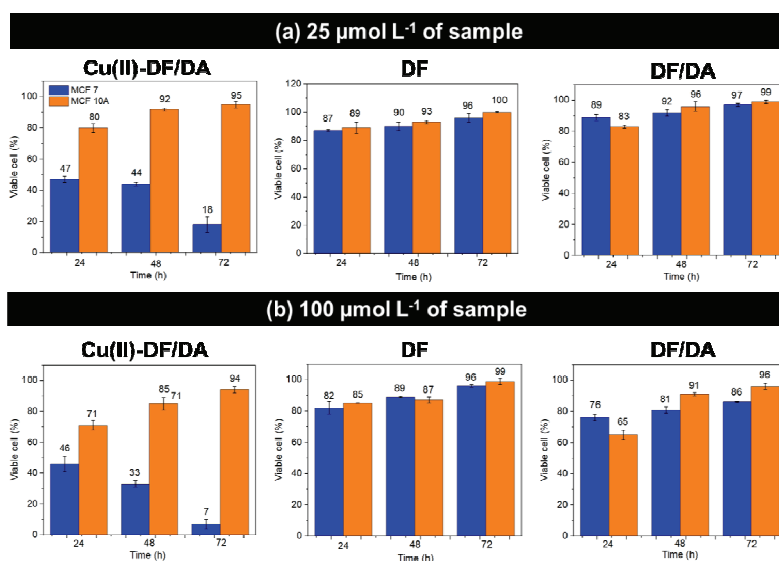


Fig. 11. Percentage of viable cells at different incubation times upon treatment with Cu(II)-DF/DA, DF and DF/DA at different concentrations.

CONCLUSION

The Cu(II)-DF/DA complex was successfully synthesised using an electrochemical approach, with the DF/DA combination serving as the ligand and Cu²⁺ as the metal centre. To confirm the formation of the desired complex, both the DF/DA compound and the Cu(II)-DF/DA complex were characterised using ATR-FTIR, NMR, XRD and UV-Vis spectroscopy. The ATR-FTIR spectra of both the DF/DA compound and the Cu(II)-DF/DA complex exhibited the presence of all functional group peaks from the raw materials. NMR analysis further confirmed that the chemical shifts of hydrogen and carbon peaks in both the compound and the complex were consistent with those of DF and DA, respectively. Additionally, EDX analysis verified the presence of Cu in the complex, indicating that Cu served as the metal centre, forming a chemical bond with the ligand. Surface morphology and particle size analyses using FESEM and TEM revealed that the synthesised Cu(II)-DF/DA complex possesses the thread-like structure with an average particle size of 4.77 ± 1.77 nm. Regarding the anticancer activity, treatment of MCF 7 cancer cells with Cu(II)-DF/DA at concentrations

of 25 and 100 $\mu\text{mol L}^{-1}$ resulted in a significant reduction in cell viability, with only 18 and 7 % of cells remaining viable after 72 h, respectively. Contrary to the given facts, nearly 90 % of normal MCF 10A cells remained viable at comparable concentrations. These findings suggest that the synthesised Cu(II)–DF/DA complex, with its small particle size of 4.77 ± 1.77 nm, is less toxic to certain normal cells, while effectively inhibiting the proliferation of selected cancer cells. Future studies could explore a wider range of Cu(II)–DF/DA concentrations to calculate the IC_{50} values and selectivity index for a more comprehensive understanding of the Cu(II)–DF/DA complexes' potency and selectivity, which would provide a more detailed assessment of their potential for targeted cancer therapy.

SUPPLEMENTARY MATERIAL

Additional data and information are available electronically at the pages of journal website: <https://www.shd-pub.org.rs/index.php/JSCS/article/view/13059>, or from the corresponding author on request.

Acknowledgements. The funding from Ministry of Higher Education Malaysia through grants Fundamental Research Grant Scheme (FRGS) with Project Code: FRGS/1/2020/STG04/USM/02/4 is gratefully acknowledged. We wish to express special thanks to the School of Chemical Sciences (USM) and Advanced Medical and Dental Institute (AMDI) USM for providing research facilities.

ИЗВОД

ЕЛЕКТРОХЕМИЈСКА СИНТЕЗА И АНТИКАНЦЕРОГЕНИ ИНХИБИТОРНИ ЕФЕКАТ КОМПЛЕКСА БАКАР(II)–ДИКЛОФЕНАК/ДЕКАНСКА КИСЕЛИНА НА ЋЕЛИЈЕ КАРЦИНОМА ДОЈКЕ MCF-7

HANISAH ABDUL RAHIM¹, NORAZZIZI NORDIN¹, BADRUL HISHAM YAHAYA², YI WEN LYE¹
и AZIZUL HAKIM LAHURI³

¹School of Chemical Sciences, Universiti Sains Malaysia 11800 Gelugor, Pulau Pinang, Malaysia, ²Regenerative Medicine Cluster, Advanced Medical & Dental Institute, Universiti Sains Malaysia, Bertam, 13200 Kepala Batas, Pulau Pinang, Malaysia и ³Department of Science and Technology, Universiti Putra Malaysia Bintulu Campus, P.O Box 396, Nyabau Road, 97008, Sarawak, Bintulu, Malaysia

У овој студији, комплекс бакар(II)–диклофенак/деканска киселина (Cu(II)–DF/DA) (бакар(II) 2-[2-(2,6-дихлороанилино)фенил]ацетамид-деканоат) синтетисана је електрохемијском методом оксидацијом бакарне аноде ради ослобађања Cu^{2+} , док су графит и KNO_3 коришћени као катода, односно помоћни електролит. Синтетисани Cu(II)–DF/DA комплекс је окарактерисан техником ATR-FTIR, NMR, XRD и UV–Vis, чиме је потврђен успех електрохемијске синтезе. Анализа морфологије површине и величине честица помоћу FESEM и TEM показала је да синтетисани Cu(II)–DF/DA комплекс има структуру налик нитима, са просечном величином честица од $4,77 \pm 1,77$ nm. Након тога, испитан је антиканцерогени инхибиторни ефекат синтетисаног комплекса на ћелије карцинома дојке MCF-7 и нормалне епителне ћелије дојке MCF-10A. Третман MCF-7 ћелија са Cu(II)–DF/DA у концентрацијама од 25 и 100 $\mu\text{mol L}^{-1}$ довео је до значајног смањења ћелијске виталности, при чему је након 72 h преживело само 18, односно 7 % ћелија. Насупрот томе, готово 90 % MCF-10A ћелија остало је витално при истим концентрацијама. Ови

rezultati ukazuju da sintetisani Cu(II)–DF/DA kompleks ima potencijal kao efikasan i selektivan antikanцерогени агенс, који показује токсичност према ћелијама карцинома, уз значајно мању према нормалним ћелијама.

(Примљено 24. септембра, ревидирано 5. новембра 2024, прихваћено 15. јануара 2025)

REFERENCES

1. N. K. Singh, A. A. Kumbhar, Y. R. Pokharel, P. N. Yadav, *J. Inorg. Biochem.* **210** (2020) 111134 (<https://doi.org/10.1016/j.jinorgbio.2020.111134>)
2. A. K. Renfrew, *Metallomics* **6**(8) (2014) 1324 (<https://doi.org/10.1039/C4MT00069B>)
3. N. Stevanović, M. Jevtović, D. Mitić, I. Z. Matić, M. D. Crnogorac, M. Vujčić, D. Sladić, B. Čobeljić, K. Anđelković, *J. Serb. Chem. Soc.* **87** (2022) 181 (<https://doi.org/10.2298/JSC211203114S>)
4. A. Alshargabi, *J. Drug Deliv. Technol.* **95** (2024) 105544 (<https://doi.org/10.1016/j.jddst.2024.105544>)
5. S. Choi, S. Kim, J. Park, S. E. Lee, C. Kim, D. Kang, *Antioxidants* **11** (2022) 1009 (<https://doi.org/10.3390/antiox11051009>)
6. L. Marinov, A. Georgiva, Y. Voynikov, R. Toshkova, I. Nikolova, M. Malchev, *Biotechnol. Biotechnol. Equip.* **35** (2021) 1118 (<https://doi.org/10.1080/13102818.2021.1953401>)
7. R. A. Poku, K. J. Jones, M. Van Baren, J. K. Alan, F. Amissah, *Cancers (Basel)* **12** (2020) 2683 (<https://doi.org/10.3390/cancers12092683>)
8. U. N. Das, *J. Adv. Res.* **11** (2018) 57 (<https://doi.org/10.1016/j.jare.2018.01.001>)
9. Y. Xu, S. Y. Qian, *Biomed. J.* **37** (2014) 112 (<https://doi.org/10.4103/2319-4170.131378>)
10. A. Guimarães, A. Venâncio, *Toxins* **14** (2022) 188 (<https://doi.org/10.3390/toxins14030188>)
11. M. Uchiyama, M. Oguri, E. H. Mojumdar, G. S. Gooris, J. A. Bouwstra, *Biochim. Biophys. Acta* **1858** (2016) 2050 (<https://doi.org/10.1016/j.bbamem.2016.06.001>)
12. M. Jóźwiak, A. Filipowska, F. Fiorino, M. Struga, *Eur. J. Pharmacol.* **871** (2020) 17293720 (<https://doi.org/10.1016/j.ejphar.2020.172937>)
13. A. Chrzanowska, P. Roszkowski, A. Bielenica, W. Olejarz, K. Stepień, M. Struga, *Eur. J. Med. Chem.* **185** (2020) 111810 (<https://doi.org/10.1016/j.ejmech.2019.111810>)
14. A. Narayanan, S. A. Baskaran, M. A. R. Amalaradjou, K. Venkitanarayanan, *Int. J. Mol. Sci.* **16** (2015) 5014 (<https://doi.org/10.3390/ijms16035014>)
15. N. Nordin, W. Z. Samad, E. Kardia, B. H. Yahaya, *Nano* **13** (2018) 1 (<https://doi.org/10.1142/S1793292018500480>)
16. R. P. Swain, R. Nagamani, S. Panda, *J. Appl. Pharm. Sci.* **5** (2015) 094 (<https://doi.org/10.7324/JAPS.2015.50715>)
17. P. B. Aiello, F. A. Borges, K. M. Romeira, M. C. R. Miranda, *Mater. Res.* **17** (Suppl. 1) (2014) 146 (<https://doi.org/10.1590/S1516-14392014005000010>)
18. N. Nordin, B. H. Yahaya, M. R. Yusop, *New J. Chem.* **42** (2018) 15127 (<https://doi.org/10.1039/C8NJ02783H>)
19. A. Yoko, G. Y. Seong, T. Tomai, T. Adschiri, *KONA Powder Part. J.* **37** (2020) 28 (<https://doi.org/10.14356/kona.2020002>)
20. R. Suhara, M. Yamagami, H. Kamitakahara, A. Yoshinaga, Y. Tanaka, T. Takano, *Cellulose* **26** (2019) 355 (<https://doi.org/10.1007/s10570-018-2027-5>)

21. E. Moctezuma, E. Leyva, C. Lara-Pérez, S. Noriega, A. Martínez-Richa, *Top. Catal.* **63** (2020) 601 (<https://doi.org/10.1007/s11244-020-01262-7>)
22. G. D. Santos Souza, A. M. Amado, A. M. R. Teixeira, P. T. C. Freire, G. D. Saraiva, G. S. Pinheiro, S. G. C. Moreira, F. F. De Sousa, C. E. S. Nogueira, *Cryst. Growth Des.* **20** (2020) 281 (<https://doi.org/10.1021/acs.cgd.9b01164>)
23. L. S. Tan, H. L. Tan, K. Deekonda, Y. Y. Wong, S. Muniyandy, K. Hashim, J. Pushpamalar, *Carbohydr. Polym. Technol. Appl.* **2** (2021) 100084 (<https://doi.org/10.1016/j.carpta.2021.100084>)
24. Y. M. Long, Q. L. Zhao, Z. L. Zhang, Z. Q. Tian, D. W. Pang, *Analyst* **137** (2012) 805 (<https://doi.org/10.1039/C2AN15740C>)
25. G. Saito, W. O. S. Wan Mohd Azman, Y. Nakasugi, T. Akiyama, *Adv. Powder Technol.* **25** (2014) 1038 (<https://doi.org/10.1016/j.apt.2014.02.003>)
26. T. D. Malevu, R. O. Ocaya, *Int. J. Electrochem. Sci.* **9** (2014) 8011 ([https://doi.org/10.1016/S1452-3981\(23\)11023-6](https://doi.org/10.1016/S1452-3981(23)11023-6))
27. N. Nordin, W. Z. Samad, M. R. Yusup, M. R. Othman, *Malaysian J. Anal. Sci.* **19** (2015) 236 (https://mjas.analis.com.my/wp-content/uploads/2018/11/Norazzizi_19_1_28.pdf).